Functional Role of the NH_2-Terminal Cytoplasmic Domain of a Mammalian A-Type K Channel

JULIE TSENG-CRANK,* JIAN-AN YAO,‡ MITCHELL F. BERMAN,§ and GEA-NY TSENG‡

From the *Molecular Biology Department, Glaxo Incorporated Research Institute, Research Triangle Park, North Carolina 27709; ‡Department of Pharmacology, Columbia University, New York, New York 10032; and §Department of Anesthesiology, Columbia University, New York, New York 10032

ABSTRACT It has been shown for a *Shaker* channel (H-4) that its NH_2-terminal cytoplasmic domain may form a "ball and chain" structure, with the "chain" tethering the "ball" to the channel while the "ball" capable of binding to the channel in its open state and causing inactivation. Equivalent structures have not been identified in mammalian *Shaker* homologues. We studied the functional role of the NH_2-terminal region of a fast-inactivating mammalian K channel, RHK1 (Kv1.4), by deleting different domains in this region and examining the resultant changes in channel properties at whole cell and single channel levels. Deleting the NH_2-terminal hydrophobic domain (domain A) or the subsequent positive charges (domain I) from RHK1 greatly slowed the decay of whole cell currents, suggesting the existence of a ball-like structure in RHK1 similar to that in the *Shaker* channel. The function of the ball appeared to be abolished by deleting domain A, while modified but maintained by deleting domain I. In the latter case, the data suggest that the positive charges needed for the function of the ball can be replaced by amino acids from a following region (domain III) that has a high positive charge density. Deleting multiple domains from the NH_2 terminus of RHK1 corresponding to the chain in *Shaker* H-4 did not induce expected changes in channel properties that might result from a shortening of a chain. A comparison of single channel kinetics of selected mutant channels with those of the wild-type channel indicated that these deletion mutations slowed whole cell currents by prolonging burst durations and by increasing the probability of reopening during depolarization. There were no changes in single channel current amplitude or latency to first opening. In conclusion, our observations indicate that the inactivation mechanism of RHK1 is similar to that of *Shaker* H-4 in that a positively charged cytoplasmic domain is important for such a process. The NH_2-terminal domain is not involved in channel activation or ion permeation process.

Address correspondence to Gea-Ny Tseng, PhD, Department of Pharmacology, Columbia University, 630 West 168th Street, New York, NY 10032.

J. GEN. PHYSIOL. © The Rockefeller University Press · 0022-1295/93/12/1057/27 $2.00
Volume 102 December 1993 1057–1083

INTRODUCTION

Armstrong and Bezanilla (1977) were the first to propose a "ball and chain" mechanism for the inactivation of Na channels. After channel activation, a positively charged cytoplasmic component ("ball") can bind to the open channel, resulting in inactivation. More recently, Hoshi, Zagotta, and Aldrich (1990) have shown that the ball and chain model is suitable for explaining the mechanism of inactivation in a *Shaker* K channel, H-4. In the *Shaker* channel, the initial 20 amino acids in the NH_2 terminus constitute the ball. Within it, the first 11 amino acids are hydrophobic. They may participate in the binding of the ball to its receptor via hydrophobic interactions. Amino acids 12–20 are hydrophilic, containing four positive and two negative charges. The net positive charge may be involved in the binding between the ball and its receptor via electrostatic interactions. Inactivation of H-4 could be disrupted by deletions or mutations in the NH_2-terminal hydrophobic domain or by reducing the net positive charge in the adjacent region (Hoshi et al., 1990). A fast inactivation could be restored in these mutant channels by adding a 20 amino acid peptide derived from the NH_2 terminus of H-4 to the cytoplasmic side of the membrane (Zagotta, Hoshi, and Aldrich, 1990). The receptor site for the ball is probably located in the inner vestibule of the pore, formed in part by the cytoplasmic loops between the fourth and fifth transmembrane domains of the channel subunits (Isacoff, Jan, and Jan, 1991). A chain domain is assigned to the region following the ball and preceding the region conserved among members of the *Shaker* family: residues 21 to about 83 of *Shaker* H-4. This region is hydrophilic with scattered positive and negative charges. It is hypothesized that the "chain" tethers the "ball" to the channel, and the length of the "chain" can influence the rate of "ball" translocation (Hoshi et al., 1990). This is based on the observations that deleting amino acids from this region accelerated channel inactivation, whereas inserting amino acids induced an opposite effect. However, this hypothesis has been challenged by some (Liebovitch, Selector, and Kline, 1992). For example, due to the influence of secondary structures deleting or inserting amino acids may not produce a proportionate change in the physical length of a chain. Other possibilities for the altered inactivation rates when mutations are made in the putative chain region, such as changes in binding affinity due to alterations in the size of the ball, can not be ruled out.

Structures equivalent to the ball and chain of *Shaker* H-4 have not been identified in mammalian homologues of *Shaker* channels. Knowledge about the molecular mechanism of K channel inactivation may be important for understanding the modulation of channel function by pathological conditions, such as extracellular K accumulation (Tseng and Tseng-Crank, 1992), and by pharmacological agents. RHK1 (Kv1.4) is a mammalian K channel that belongs to the *Shaker* family (Tseng-Crank, Tseng, Schwartz, and Tanouye, 1990; Chandy, 1991). Unlike many other mammalian members of this family, RHK1 shows fast inactivation kinetics. RHK1 displays prominent divergence from the other mammalian homologues in its first 174 amino acids. This suggests that the NH_2-terminal region may play a crucial role in the inactivation process of RHK1. A comparison of the charge distribution in the NH_2 termini of RHK1 and H-4 is shown in Fig. 1 (*top*). We have divided the first 174 residues of RHK1 into several domains and labeled them as A to E and I to IV

(Table I). This division was based on the hydrophobicity or the charge densities in this region. Domain A includes the initial 25 amino acids that are mainly hydrophobic. This is followed by domain I that is hydrophilic, containing five positive and two negative charges. Domains B, II, C, D, and E are mainly hydrophobic. Domain III is highly positively charged, whereas domain IV contains a high density of negative charges. The boundaries of these domains are specified in Table I. In analogy to the structure of H-4, domains A and I of RHK1 may constitute the ball, and the domains following the ball but preceding the conserved region may constitute the chain (Fig. 1).

In the present study, we deleted different domains from the NH_2 terminus of RHK1 singly or in combination, and examined the resulting changes in channel function at both whole cell and single channel levels. The following questions were addressed: (*a*) can the function of a ball and a chain be confirmed in RHK1? (*b*) Does the NH_2-terminal region participate in channel function other than inactivation (Stocker, Stuhmer, Wittka, Wang, Muller, Ferrus, and Pongs, 1990)? (*c*) What is the function of the high charge densities in domain III and domain IV? And (*d*) what aspects of channel gating are modified by deleting different domains from the NH_2 terminus of RHK1? A preliminary report has appeared in an abstract form (Yao, Tseng-Crank, Lipka, Berman, and Tseng, 1992).

MATERIALS AND METHODS

In Vitro Mutagenesis

Site-directed mutagenesis was carried out following a modified procedure of Kunkel (1985), as described previously (Tseng and Tseng-Crank, 1992). Oligonucleotides designed with various mutations were synthesized with a DNA synthesizer (380B, Applied Biosystems, Foster City, CA), and purified with HPLC chromatography (Hewlett Packard Series II, 1090 Liquid Chromatograph). Table I lists the NH_2-terminal sequences of deletion mutants included in this study. The oligonucleotide sequences (from 5′ to 3′) used for generating the mutants were as follows: deletions of single domains: Del A (residues 3–25 from domain A removed): CCCCAAACTACCACCATGGAGAGGGCTCGAGAGAGG, Del I (residues 26–37 removed): GGTTATGCTGCCCAGGCCGCAGCTGCAGCTCTGGC, Del B (residues 38–61 removed): CTTGCTCACTCCAGGCACCATCATCATCAG, Del II (residues 62–65 removed): GGTTCTGGTGGAGGCCCCCAGACACGTGG, Del III (residues 80–98 removed): GATCCTCAAGGAAGCCAGAGCAGTTTTCCTC, Del D (residues 99–113 removed): CTCCACCACAGGGAAGAGAAGATCCTTAGG, Del IV (residues 114–139 removed): CTGATGCCCAGTGGCTCTTTTTACTATAGTGAAGAG, and Del E (residues 140–173 removed): GAAGAGGAGGGAAGGGACTGTTGTGAACGCGTG; deletions of multiple domains: Del IB (residues 26–61 removed) derived from Del I with the oligonucleotide sequence GGTTATGCTGCCCAGGCCCACCATCATCATCAG, Del BII (residues 38–65 removed) derived from Del II with the oligonucleotide sequence GCTCACTCCAGGCAGACACGTGGG, Del IIC (residues 62–79 removed) derived from Del II with the oligonucleotide sequence GGTGGAGGCCCCCGAGGTAGTCGG, Del IBIIC (residues 26–79 removed) derived from Del IB with the oligonucleotide sequence GGTTATGCTGCCCAGGCCCGAGGTAGTCGGAGG.

Three to five mutants per mutagenesis reaction were confirmed by restriction fragment length reduction and DNA sequencing. Two independent mutants for each mutation were prepared for in vitro transcription and *Xenopus* oocyte expression. Data from the two independent mutants correlated with each other and were pooled.

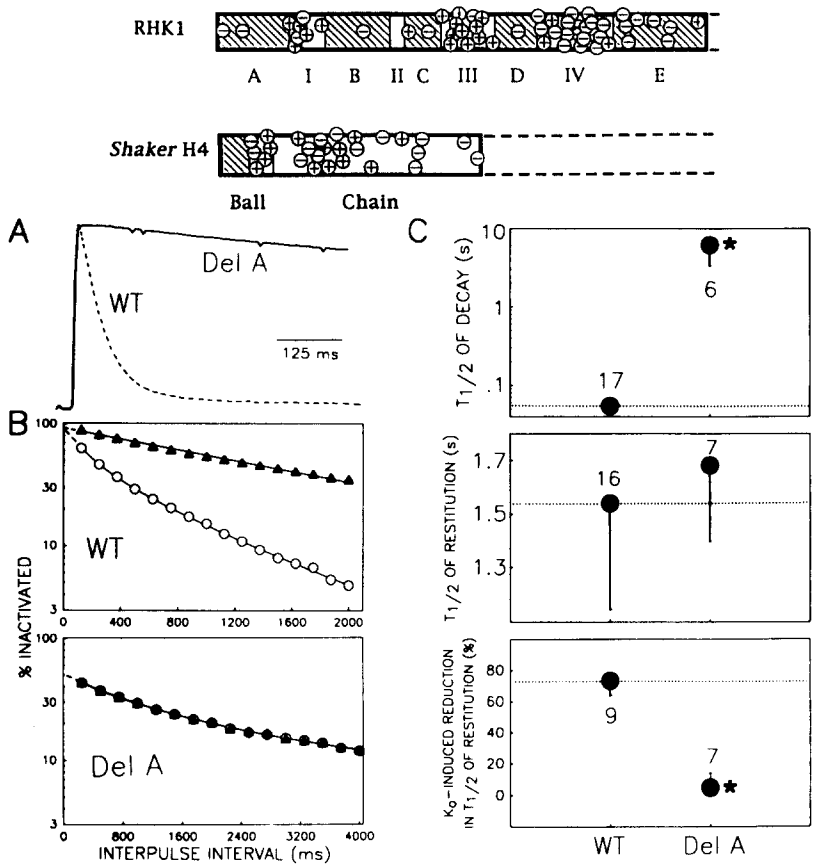

FIGURE 1. (*Top*) Comparison of charge distribution in the NH_2 termini of RHK1 and *Shaker* H-4. Schematic diagrams of the NH_2-terminal divergent regions of these two channels are shown, with the following regions conserved among *Shaker* family members denoted by broken lines. The charges are marked as plus or minus signs in circles. The NH_2 terminus of the *Shaker* channel is divided into "ball" (residues 1–20) and "chain" (residues 21–83) domains according to Hoshi, Zagotta, and Aldrich (1990). The NH_2 terminus of RHK1 is also divided into different domains as illustrated. The boundaries between these domains are listed in Table I. (*A*) Comparison of the rate of decay between the wild-type RHK1 (*WT*) and a deletion mutant in which amino acids 3–25 from domain A had been removed (*Del A*). The currents were induced by depolarization steps from −80 to +20 mV. The leak and capacitive currents were subtracted using a scaled template created by averaging 20 traces induced by a step from −80 to −70 mV. The currents were scaled to the same peak or initial current amplitudes and superimposed. (*B*) Comparison of time courses of recovery from inactivation (restitution) and effects of elevating $[K]_o$ on restitution between WT and Del A. The restitution time courses were measured in the following manner. From a holding voltage of −80 mV, double pulses each to +20 mV with a varying interpulse interval (125–4,000 ms) were applied every 15 s (*WT*) or 20 s (*Del A*). The duration of each of the double pulses was 500 (*WT*) or 5,000 (*Del A*) ms. After leak subtraction, the peak current amplitudes during the first (I_1) and the second (I_2) pulses were measured, and the difference between the two was normalized by I_1 to give an estimate of the percent of channels remaining inactivated after the interpulse interval (*% inactivated*). The time courses of

cDNA In Vitro Transcription and Oocyte Expression

The cDNA sequences of RHK1 and mutant channels in pBluescript vector (Stratagene Inc., La Jolla, CA) were used to prepare DNA templates for in vitro cRNA synthesis as described before (Tseng-Crank et al., 1990). In brief, the templates were linearized by *Hind III* and transcription reactions were carried out using the TransProbe kit from Pharmacia LKB Biotechnology, Inc. (Piscataway, NJ) and T7 RNA polymerase in the presence of a "cap analogue" [$m^7G(5')_{ppp}(5')G$]. For each transcription reaction, the quality of the cRNA product was checked by denaturing agarose gel electrophoresis and autoradiography. The cRNA was resuspended in RNAse-free water for microinjection. *Xenopus* oocytes were released from follicular cell layers by collagenase treatment. 4–6 h after isolation, oocytes were microinjected with a cRNA solution at 30–50 nl each. The oocytes were incubated at 18°C in an ND96 solution (composition in mM: NaCl 96, KCl 2, $CaCl_2$ 1.8, $MgCl_2$ 1.0, HEPES 5, Na-pyruvate 2.5, pH 7.5 with NaOH), supplemented with penicillin (100 U/ml) and streptomycin (100 μg/ml). Membrane currents were studied 2–6 d after injection.

Electrophysiological Experiments

For whole-cell voltage clamp experiments, the oocytes were placed in a tissue chamber and superfused at room temperature (21–23°C) with ND96 solution at a rate of ~3 ml/min. Membrane currents were studied using the conventional two-microelectrode voltage clamp technique with an AxoClamp-2A amplifier (Axon Instruments, Foster City, CA). Both voltage and current electrodes were filled with 3 M KCl solution and had tip resistances of 1–2 MΩ. A grounded shield was placed between the two electrodes to decrease capacitance coupling. During current recordings, the external solution was changed to a nominally Ca-free ND96 solution ($CaCl_2$ replaced by $MgCl_2$) to minimize interference from endogenous Ca-activated Cl currents (Bolton, Dascal, Gillo, and Lass, 1989).

For single channel recording, oocytes with vitelline membrane removed (Methfessel, Witze-

---

restitution were measured at 2 (*filled triangles*) and then 20 (*open circles*) mM $[K]_o$. For WT, the restitution time course at 2 mM $[K]_o$ could be well fitted with a single exponential function: $y(t) = y(0)\exp(-t/\text{tau})$, where $y(0)$ and $y(t)$ are the percentages of channels inactivated at time zero (the end of the first pulse) and after an interpulse interval "t," respectively; "tau" is the time constant of restitution. At 20 mM $[K]_o$, the restitution time course of WT required a double exponential function for a good fit: $y(t) = y_1(0)\exp(-t/\text{tau}_1) + y_2(0)\exp(-t/\text{tau}_2)$, where tau_1 and tau_2 are the time constants of the fast and slow components, whose fractions at time zero are denoted by $y_1(0)$ and $y_2(0)$, respectively. For Del A, the 5,000 ms first pulses induced about 50% inactivation. The restitution of the inactivated component of Del A followed an apparent double exponential time course at both 2 and 20 mM $[K]_o$. In each panel, the values of "% inactivated" are plotted against interpulse intervals on a semilogarithmic scale. Data are superimposed on lines or curves calculated from single or double exponential function with the best-fit parameter values. (*C*) (*top*) Comparison of the half-time ($T_{1/2}$) of current decay at +20 mV between WT and Del A. Note that the ordinate uses a logarithmic scale. (*Middle*) Comparison of the half-time of recovery from inactivation ($T_{1/2}$ of restitution) between WT and Del A. $T_{1/2}$ of restitution was determined from the restitution time course. For Del A, this parameter refers to the time when 50% of the inactivated channels recovered from inactivation. (*Bottom*) Comparison of the % reduction in $T_{1/2}$ of restitution induced by elevating $[K]_o$ from 2 to 20 mM between WT and Del A. Shown are means (*closed circles*) and standard deviation bars, with the numbers of observations marked adjacent to the symbols. For $T_{1/2}$ of decay of WT, the standard deviation bar is smaller than the symbol. *: $P < 0.05$ relative to WT.

TABLE I

NH_2-Terminal Sequences of RHK1 Wild-Type and Deletion Mutant Channels

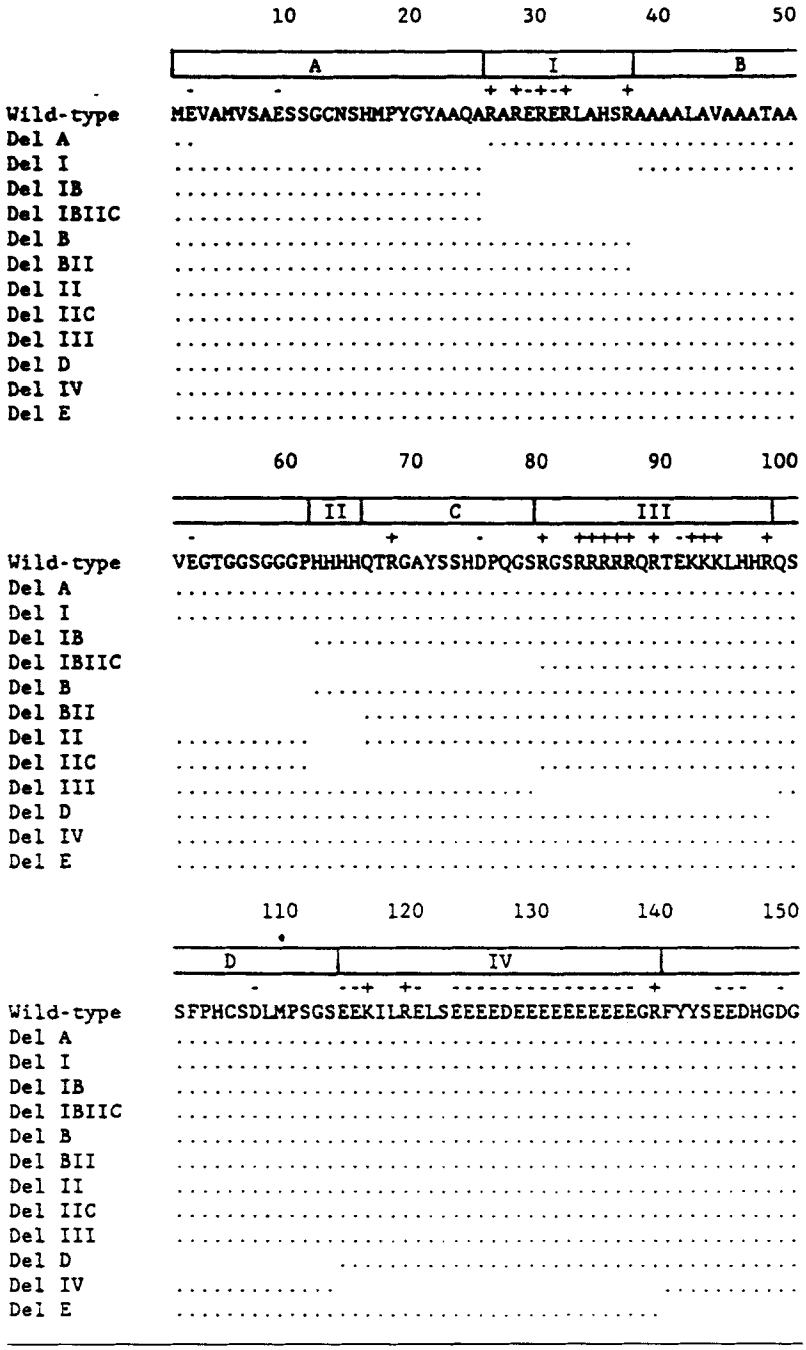

mann, Takahashi, Mishina, Numa, and Sakmann, 1986) were bathed in a high [K] solution that brought the transmembrane voltage to approximately zero (in mM: KCl 140, $MgCl_2$ 2, EGTA 11, HEPES 10, pH 7.1 with KOH). The pipettes were coated with Sylgard (Dow Corning) to near the tip. The pipette tips were filled with ND96 solution and had tip resistances of 2–15 MΩ. Single channel currents were recorded in the cell-attached patch configuration (Hamill, Marty, Neher, Sakmann and Sigworth, 1981) using an AxoPatch-1C amplifier (Axon Instruments).

Voltage clamp protocol generation and data acquisition were controlled by an IBM/AT-compatible computer through a software, pClamp (Axon Instruments), via a 12 bit D/A and A/D converter (TL-1 DMA Interface, Axon Instruments). Currents were low-pass filtered with an eight-pole Bessel filter at 2 kHz (Frequency Devices, Inc., Haverhill, MA), digitized on-line and stored on disk for off-line analysis. The sampling intervals for whole cell currents ranged

TABLE I.
(continued)

	160 170
	E
	- -- + -
Wild-type	CSTYDLLPQDDGGGGGYSSVRYSD
Del A	.....
Del I	.....
Del IB	.....
Del IBIIC	.....
Del B	.....
Del BII	.....
Del II	.....
Del IIC	.....
Del III	.....
Del D	.....
Del IV	.....
Del E	.

The amino acid sequence of the NH_2-terminal 174 residues of the RHK1 wild-type channel is listed using the one-letter code, with the sequences of various deletion mutants aligned below. The numbers on top denote those of the residues in the wild-type channel. The "+" and "−" signs above the amino acid sequences mark positively and negatively charged residues. The regions designated as domains A, I, B, II, C, III, D, IV, and E and the boundaries between them are shown above the sequences. For each of the deletion mutants, "..." represent residues identical to those of the wild-type channel, while an empty space indicates the sequence removed.

from 0.5 to 7 ms, depending on the purposes of the voltage clamp protocols and the rate of decay of the current under study. The sampling interval for single channel currents was 0.1 ms.

Data Analysis

Data analysis was mainly done with the pClamp programs. For whole cell data analysis, PeakFit (Jandel Scientific, Corte Madera, CA) was also used to fit the activation curves with a double sigmoidal function (see Table II legend), and the time course of channel recovery from inactivation with a single or double exponential function. When analyzing single channel currents, the data were further processed by a digital filter (Fetchan of pClamp) so that the final

filter frequency was 1 kHz (Colquhoun and Sigworth, 1983). To avoid interference in the measurements of single channel current amplitude and kinetics due to overlapped openings, current traces containing overlapping events were excluded from analysis. The number of active channels in a patch was estimated by observing the maximum number of simultaneously open channels when the patch membrane potential was stepped from a very negative holding voltage (−100 to −120 mV) to a strongly depolarized voltage (+40 to +60 mV). Most of the patches considered here contained two or three active channels. The holding voltage (−50 to −120 mV) and interpulse interval (2–10 s) were chosen so that ~25% of the sweeps were null (without channel openings). Under these conditions, when channel activities were seen they were mostly openings to the single level. Leak and uncompensated capacitive currents were digitally subtracted using leak templates constructed by averaging null sweeps. Single channel current amplitude was determined from amplitude histograms. The currents were then idealized using a 50% amplitude criterion to detect opening and closing transitions (Colquhoun and Sigworth, 1983). We did not attempt to correct for missed events.

Specific voltage clamp protocols and data analyses will be described in the corresponding figure or table legends. Wherever applicable, data were averaged and presented as mean ± SD. Statistical significance was tested by unpaired, two-sided *t*-test.

RESULTS

The NH_2-terminal sequences of the wild-type (WT) RHK1 and deletion mutant channels are listed in Table I. Deleting domain B, II, D, or E alone or deleting domains BII or IIC simultaneously from RHK1 did not induce appreciable changes in the rate of current decay during depolarization (data not shown). On the other hand, deleting domain A (Fig. 1), I (Fig. 6), III or IV (Fig. 8) alone or deleting domain I and its adjacent regions (B, II and C, Fig. 6) caused marked changes in the kinetic properties of RHK1. Therefore, the present study was focused on the effects of these latter mutations on channel function.

We characterized and compared the following channel properties at the whole cell level: rate of decay during depolarization, rate of recovery from inactivation (restitution), effects of elevating $[K]_o$ on restitution, and voltage-dependence of activation. The rationale for these measurements and their interpretation will be presented in the Discussion section. For selected mutant channels (Del A, Del IB, and Del III), we also recorded single channel currents from cell-attached patches and compared their properties to those of WT current to determine what aspects of channel gating were modified by these NH_2-terminal deletions.

Effects of Deleting Domain A

Whole cell current. Fig. 1 *A* compares the time courses of WT and Del A recorded at +20 mV. After rising to a peak, the WT current displayed a fast decay that followed a single exponential time course (Tseng-Crank et al., 1990). On the other hand, Del A current showed very little decline at the same time scale. Prolonging the depolarization pulse revealed a complicated decay time course of Del A that needed at least three exponential components for a reasonable fit (Tseng and Tseng-Crank, 1992). Due to the qualitative difference in the time course of decay, we chose to use the half-time ($T_{1/2}$) of decay for a comparison between the two. The average $T_{1/2}$ of decay at +20 mV was 0.055 ± 0.020 s for WT and 6.1 ± 2.8 s for Del A (Fig. 1 C, *top*). Thus, deleting domain A from RHK1 caused a 110-fold prolongation of $T_{1/2}$ of decay.

Fig. 1 *B* shows representative time courses of restitution of WT and Del A and the effects of elevating $[K]_o$ on restitution. The voltage clamp protocol and data analysis are described in Fig. 1 legend. For WT, the duration of the conditioning pulse (500 ms) was long enough to cause a complete inactivation. On the other hand, the inactivation of Del A was so slow that even with a conditioning pulse of ten times duration (5 s) the inactivation was only ~50% complete. Therefore, for Del A the restitution of the component inactivated by the first pulse was used for analysis and comparison with WT. At 2 mM $[K]_o$, WT channels recovered from inactivation with a single exponential time course, as evidenced by the linear semilogarithmic plot shown by the filled triangles in the upper panel of Fig. 1 *B*. The time course of restitution of Del A was not single exponential, as suggested by the curvilinear semilogarithmic plot shown in the lower panel of Fig. 1 *B*. The curve superimposed on the Del A data points in Fig. 1 *B* was calculated based on a double exponential function. Due to the qualitative difference in the time course of restitution, we chose to use the half-time ($T_{1/2}$) of restitution for a comparison between the two. The $T_{1/2}$ of restitution were 1.5 ± 0.4 s for WT, and 1.7 ± 0.3 s for Del A (Fig. 1 *C, middle*). Therefore, in sharp contrast to the marked difference in the rate of decay during depolarization, there was no significant difference in the $T_{1/2}$ of restitution between WT and Del A.

Elevating $[K]_o$ accelerated the restitution of WT. As shown in the upper panel of Fig. 1 *B*, after an interpulse interval of 2 s, 40% of the WT channels still remained inactivated at 2 mM $[K]_o$, but only 4% was inactivated when $[K]_o$ was raised to 20 mM. On average, such a change in $[K]_o$ reduced the $T_{1/2}$ of restitution of WT by 73.2 ± 9.5% (Fig. 1 *C, bottom*). A similar phenomenon has been described for the *Shaker* H-4 channel (Demo and Yellen, 1991). As suggested by Demo and Yellen (1991) and by us (Tseng and Tseng-Crank, 1992), elevating $[K]_o$ may accelerate the exit of the inactivation gate (ball) from the pore at negative voltages by an electrostatic repulsion, thus speeding the restitution. Del A's restitution time courses at 2 and 20 mM $[K]_o$ were superimposable (lower panels of Fig. 1 *B* and *C*), indicating that removing domain A from RHK1 abolishes the effects of external K ions on restitution.

We constructed activation curves to determine whether deleting domain A could influence the voltage-dependence of channel gating. The voltage clamp protocols and data analysis are described in Table II legend. As shown previously, the activation curves of both RHK1 and Del A could not be described by the conventional simple Boltzmann equation, but could be well fitted with a double sigmoidal function (Tseng and Tseng-Crank, 1992). The two channels had similar activation curves. For both, the negative component of the activation curve accounted for 50% of the conductance, with a half-maximum voltage of −36 to −37 mV and a slope factor of 7 mV. The positive component had a slope factor of 19 mV and a half-maximum voltage of 7 (WT) or 18 (Del A) mV (Table II).

Single channel current. Fig. 2 illustrates representative single channel currents of WT and Del A recorded at +40 mV. For WT, openings clustered at the beginning of the pulse. The channel often opened and closed several times (bursting) before entering a long-lived closed (inactivated) state. Reopenings from the inactivated state were rare. For Del A, the channel activity was high throughout the duration of the

400 ms depolarization pulse. The channel opened and closed many times before entering a longer-lived closed state. Reopenings from this state were frequent. The bottom plots depict the ensemble averages from the same patches. The ensemble averages shown here have been converted to the time courses of changes in the open probability (Fig. 2, legend). The characteristics of the ensemble averages (i.e., fast decaying WT and sustained Del A) reflected those of the single channel currents, and are similar to the whole cell current recordings (Fig. 1 *A*).

For WT, the marked difference in the closed intervals in the single channel recordings suggests that there are at least two closed states, a short-lived one

TABLE II

Comparison of Voltage-dependence of Activation Between the Wild-Type RHK1 (WT) and NH_2-Terminal Deletion Mutants

	A_1	V_1	k_1	V_2	k_2
WT (11)	0.50 ± 0.08	−37.4 ± 3.1	7.1 ± 1.8	+6.8 ± 7.4	19.8 ± 2.5
Del A (3)	0.46 ± 0.05	−36.4 ± 0.3	6.8 ± 0.5	+18.0 ± 2.2	18.6 ± 0.5
Del I (6)	0.49 ± 0.03	−34.4 ± 5.1	7.8 ± 1.1	+12.1 ± 5.0	18.1 ± 1.6
Del IB (5)	0.51 ± 0.07	−34.7 ± 3.0	7.6 ± 0.5	+7.1 ± 7.0	18.4 ± 1.1
Del IBIIC (3)	0.50 ± 0.02	−29.3 ± 5.3	8.0 ± 0.4	17.0 ± 6.9	17.8 ± 0.5
Del III (8)	0.50 ± 0.01	−32.5 ± 5.4	8.4 ± 0.6	+14.3 ± 7.7	18.1 ± 0.8
Del IV (6)	0.45 ± 0.07	−32.5 ± 1.5	8.4 ± 0.3	+13.4 ± 8.8	18.1 ± 1.4

The activation curve was determined using two protocols. For the first protocol, the peak current-voltage (I-V) relationship was determined over a range of test voltages (V_t) from −70 to +70 mV in 10 mV increments. The peak current amplitude at each V_t was divided by the driving force ["$V_t - E_K$," where E_K was assumed to be −100 mV (Tseng-Crank, Tseng, Schwartz, and Tanouye, 1990)] to give an estimate of the peak chord conductance at V_t. The peak chord conductance was normalized to that at +70 mV to give an estimate of the fraction of channels activated at V_t. For the second protocol, the tail current amplitudes at −60 mV induced by short depolarizing prepulses to different test voltages (V_t) were measured, and normalized to that induced by a V_t of +70 mV. Depending on V_t, the prepulse lasted 10–20 ms during which the current reached a peak without appreciable decay. The normalized tail I–V relationship gave a second estimate of the fractions of channels activated at various V_t. The relationship between the fraction of channels activated and V_t obtained by either method was fitted with the following equation (Tseng and Tseng-Crank, 1992):

$$\text{fraction of channels activated} = A_1/\{1 + \exp[(V_1 - V_t)/k_1]\} + (1 - A_1)/\{1 + \exp[(V_2 - V_t)/k_2)\}$$

where A_1 represents the component of channels activated in the more negative voltage range, V_1 and k_1 are the half-maximum activation voltage and slope factor of this component. V_2 and k_2 are the corresponding parameters of the component activated in the more positive voltage range. There were no noticeable differences in the activation curves obtained by these two methods. Therefore, the data were pooled and reported here. The numbers of observations are shown in parentheses.

corresponding to the closed intervals within bursts, and a long-lived one corresponding to the closed intervals between bursts (Magleby and Pallotta, 1983; Solc and Aldrich, 1990). For Del A, a similar distinction was discernable, although much less prominent than the WT channel. We defined bursts by a "criterion duration" (Magleby and Pallotta, 1983; Solc and Aldrich, 1990): any closed intervals longer than the criterion duration were assigned to represent gaps between bursts, while closed intervals shorter than or equal to the criterion duration represented gaps

within bursts. This criterion duration was set at five times the fastest time constant of the closed time distribution of each patch (Fig. 4 *B*). The rationale for this method and possible error in our data analysis will be discussed (see Discussion). For the WT patch shown in Fig. 2 *A*, the criterion duration was set at 1.4 ms. This gave a mean

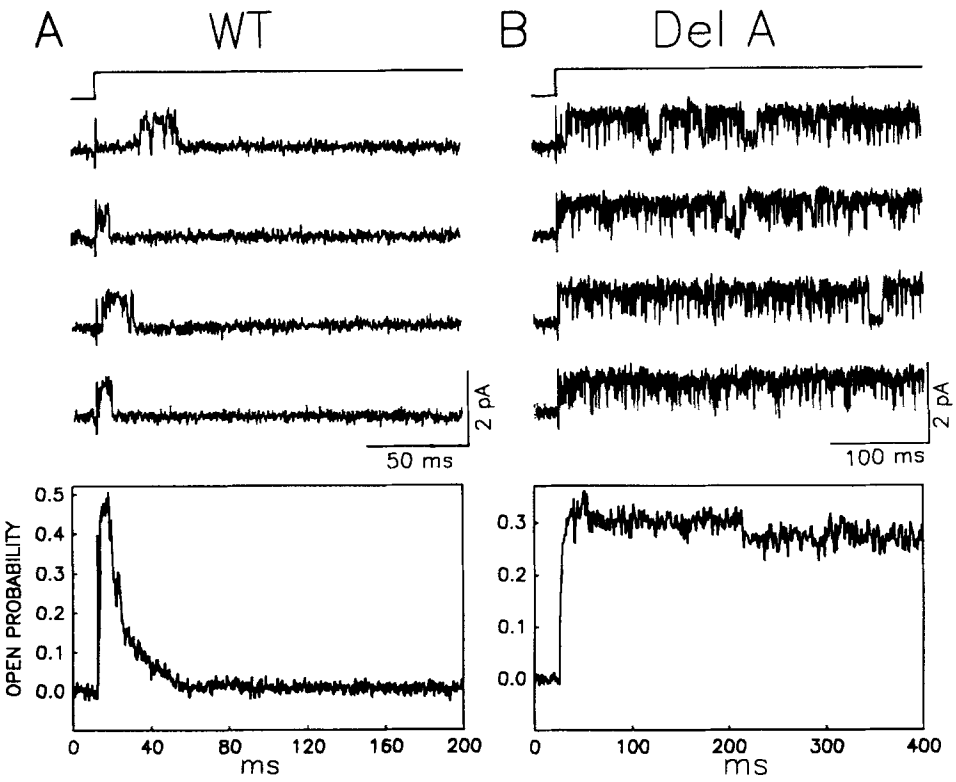

FIGURE 2. Single channel currents of wild-type RHK1 (*WT, A*) and Del A (*B*). In each panel, four representative original current traces recorded at +40 mV are shown. The depolarization steps were repeated every 10 s from a holding voltage (V_h) of −100 to −120 mV (*WT*) or −50 to −70 mV (*Del A*). The onset of the depolarization pulses is indicated above. V_h was adjusted so that ~25% of the sweeps were null, and openings were mostly to the single level. The leak and uncompensated capacitive currents were subtracted using templates created by averaging null traces. Note the difference in time calibrations. The plot on the bottom of each panel denotes the time course of changes in the open probability calculated by dividing the ensemble average current by the product of number of channels in the patch (three for both) and single channel current amplitude (0.64 pA for WT and 0.66 pA for Del A). Data were from the same patches as the original current traces. The ensembles were averaged from 154 traces for WT and 55 traces for Del A.

burst duration of 11.4 ms and a mean number of openings per burst of 4. For the Del A patch shown in Fig. 2 *B*, the criterion duration was 1.3 ms. The mean burst duration was 56 ms and the mean number of openings per burst was 14. Determined in the same fashion, the average values of mean burst duration and mean number of

openings per burst were 16.6 ± 8.2 ms and 8.3 ± 3.9 for WT, 48.7 ± 10.1 ms and 16.8 ± 3.2 for Del A (Table III). Therefore, the bursts of Del A tended to last longer than those of WT. This prolongation was partially due to an increase in the number of openings per burst, and partially due to an increase in the mean channel open time (see below).

Fig. 3 illustrates the average single channel current-voltage (i-V) relationship of WT. In the voltage range examined (+20 to +60 mV), the i-V relationship was linear with a slope conductance of 9.3 pS. Fig. 3 also shows that the average single channel current amplitudes of Del A at +40 and +60 mV were similar to those of WT,

TABLE III

Comparison of Single Channel Properties Between the Wild-Type RHK1 (WT) and NH_2-Terminal Deletion Mutants‡

	WT	Del A	Del IB	Del III
Current amplitude (pA)	0.63 ± 0.08	0.66 ± 0.10	0.74 ± 0.05	0.73 ± 0.10
	(10)	(10)	(6)	(4)
Mean open time (ms)§	1.4 ± 0.3	1.9 ± 0.3*	2.1 ± 0.4*	2.2 ± 0.2*
	(9)	(7)	(6)	(4)
Mean closed time within bursts (ms)‖	0.36 ± 0.08	0.32 ± 0.05	0.34 ± 0.04	0.32 ± 0.04
	(9)	(7)	(6)	(4)
Median first latency (ms)¶	3.7 ± 1.3	3.1 ± 0.9	2.5	2.8 ± 0.2
	(4)	(6)	(2)	(3)
Mean burst duration (ms)**	16.6 ± 8.2	48.7 ± 10.1*	28.4 ± 2.9*	32.6 ± 9.0*
	(6)	(4)	(4)	(4)
Mean number of openings per burst**	8.3 ± 3.9	16.8 ± 3.2*	9.9 ± 1.0*	9.5 ± 3.9*
	(6)	(4)	(4)	(4)

‡All measurements were made at +40 mV. Shown are mean ± SD. Values in parentheses are numbers of observations. *$P < 0.05$, relative to WT by unpaired, *t*-test. §The mean open time was the time constant of a single exponential fit to the open time histogram. ‖The mean closed time within bursts was the time constant of the fast component of a double exponential fit to the histogram of closed times ≤ 8 ms. ¶The median first latency was obtained in the following manner. The cumulative first latency distribution, which specified the probability that the latency to first opening was longer than the time on the abscissa, was corrected for the number of channels present in the patch (Aldrich, Corey, and Stevens, 1983). The time at which 50% of the first openings had occurred was taken as the median first latency. **Bursts were defined by a criterion duration: a closed interval longer than this criterion duration was taken as a termination of a burst. For each patch, the criterion duration was set at five times the mean closed time within bursts. The mean burst duration and mean number of openings per burst represented the algebral means of respective parameters.

suggesting that deleting domain A from RHK1 did not alter the ion permeation process of the channel.

The single channel kinetics of WT and Del A within bursts were examined by analyzing the distributions of their open times and closed times. The open time histograms of both WT and Del A could be well fitted with a single exponential function (Fig. 4 *A*, *left*). Deleting domain A caused a slight but significant prolongation of the mean channel open time (1.4 ± 0.3 ms for WT vs 1.9 ± 0.3 ms for Del A, $P < 0.03$; Fig. 4 *A* [right] and Table III). The left panels of Fig. 4 *B* illustrate closed time histograms from the same patches as in *A*. The analysis was restricted to closed

times shorter than 8 ms. A double exponential function provided a good fit to the closed time histograms of both WT and Del A. The shorter time constant was 0.35 ms for WT and 0.37 ms for Del A. The average value of this time constant was 0.36 ± 0.08 ms for WT, and 0.32 ± 0.05 ms for Del A (right panel of Fig. 4 *B* and Table III). Thus, deleting domain A did not affect the mean closed time within bursts.

Fig. 5 *A* compares the latency to first opening (first latency) between WT and Del A. Shown are the cumulative distributions of first latency, which specify the probability that the first opening occurs at a time later than the time on the abscissa. These distributions have been corrected for the number of channels in the patches (Aldrich, Corey, and Stevens, 1983). For both channels, there was a distinct initial delay before first openings occurred, indicating that channels needed to traverse more than one closed state before opening (Zagotta and Aldrich, 1990). The two distributions were almost superimposable. We quantified the first latency from its distribution by measuring the median value, which was the time when 50% of the first openings had occurred (Zagotta and Aldrich, 1990). This value was 5 ms for both patches shown in

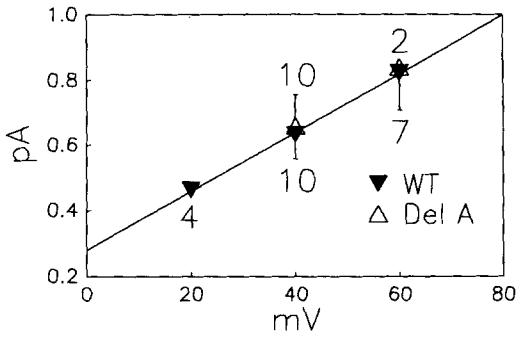

FIGURE 3. Single channel current-voltage relationship of WT RHK1 and Del A. The single channel current amplitudes were determined from amplitude histograms measured from current traces that contained only one level of openings. Shown are means (*symbols*) and standard deviation bars with the numbers of observations marked. Numbers below the symbols are for WT and those above the symbols are for Del A. For the WT data point at +20 mV, the standard deviation bar is smaller than the symbol. The slope conductance of WT was 9.3 pS estimated by regression analysis (*superimposed line*).

Fig. 5 *A*. Determined in the same manner, the average values of median first latency were 3.7 ± 1.3 ms for WT and 3.1 ± 0.9 ms for Del A ($P > 0.4$, Table III). These observations suggest that the rate of channel activation was not altered by deleting domain A from RHK1, consistent with the notion that deleting domain A did not affect the voltage dependent activation process of the channel (Table II).

To explain the reduction in the rate of current decay caused by deleting domain A observed at the whole cell level, we considered single channel properties that have been shown to be important for determining the time course of macroscopic current: the latency to first opening, the burst duration and the probability of channel reopening (Aldrich et al., 1983; Yue, Lawrence, and Marban, 1989). As shown above, the latency to first opening was not altered by deleting domain A. Therefore, we could rule out this factor as a cause for the slowed decay of Del A. There was a threefold prolongation of the burst duration in Del A relative to WT (Table III). This was not sufficient to account for the 110-fold increase in $T_{1/2}$ of decay in Del A (Fig. 1 *C*). Therefore, an important factor that slowed the decay of whole cell current in

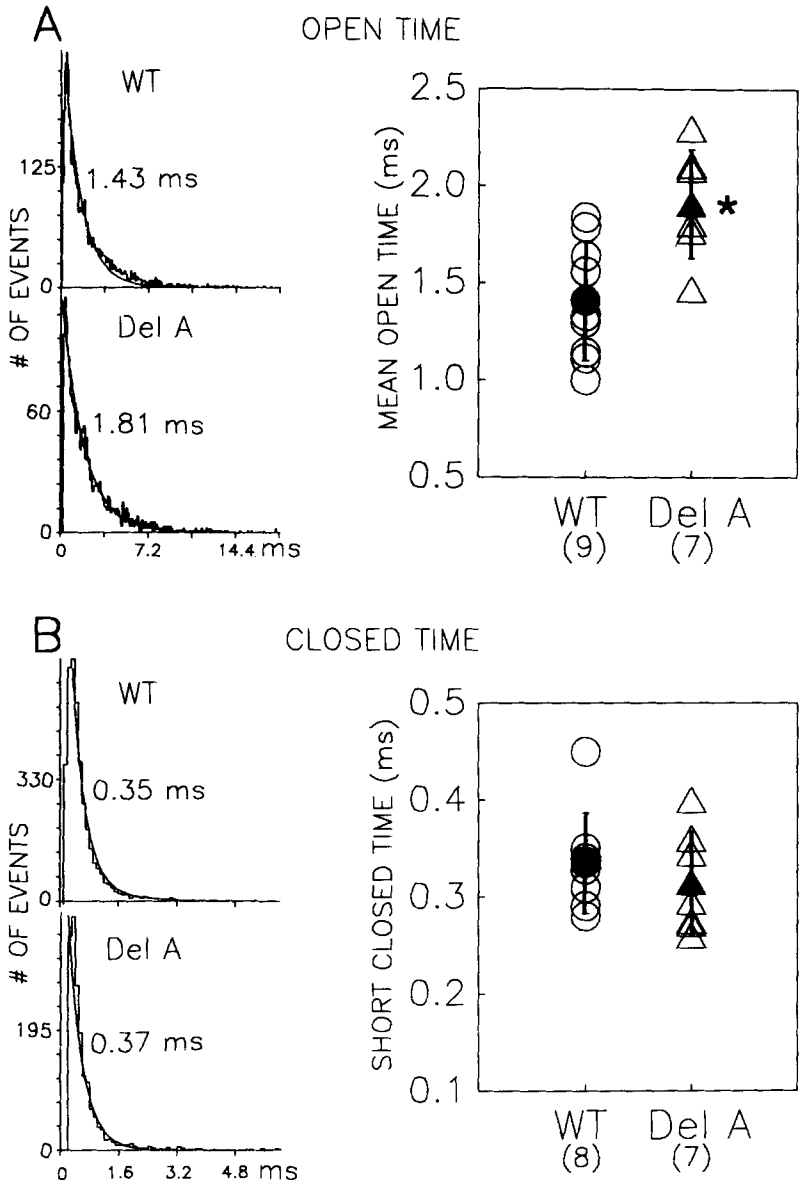

FIGURE 4. Comparison between WT and Del A of the mean open time (*A*) and mean closed time within bursts (*B*). The single channel currents were recorded at +40 mV. The traces with only one level of channel openings were leak-subtracted and idealized using a 50% amplitude criterion to detect opening and closing transitions. The idealized records were used for constructing open time and closed time histograms. The histograms were fitted with a single exponential (*open time*) or double exponential (*closed time*, ≤ 8 ms) function using a nonlinear least-squares method. The left panels illustrate representative open time and closed time histograms of WT and Del A. The superimposed curves were calculated from the appropriate function with the best-fit parameter values. Also shown are the mean open times and mean short closed times. Data in the left panels of *A* and *B* were from the same patches. The right panels show data summary with open symbols representing data from individual experiments (the number of experiments are shown in the parentheses along the abscissa), while closed symbols representing mean values along with standard deviation bars. (*) $P < 0.03$.

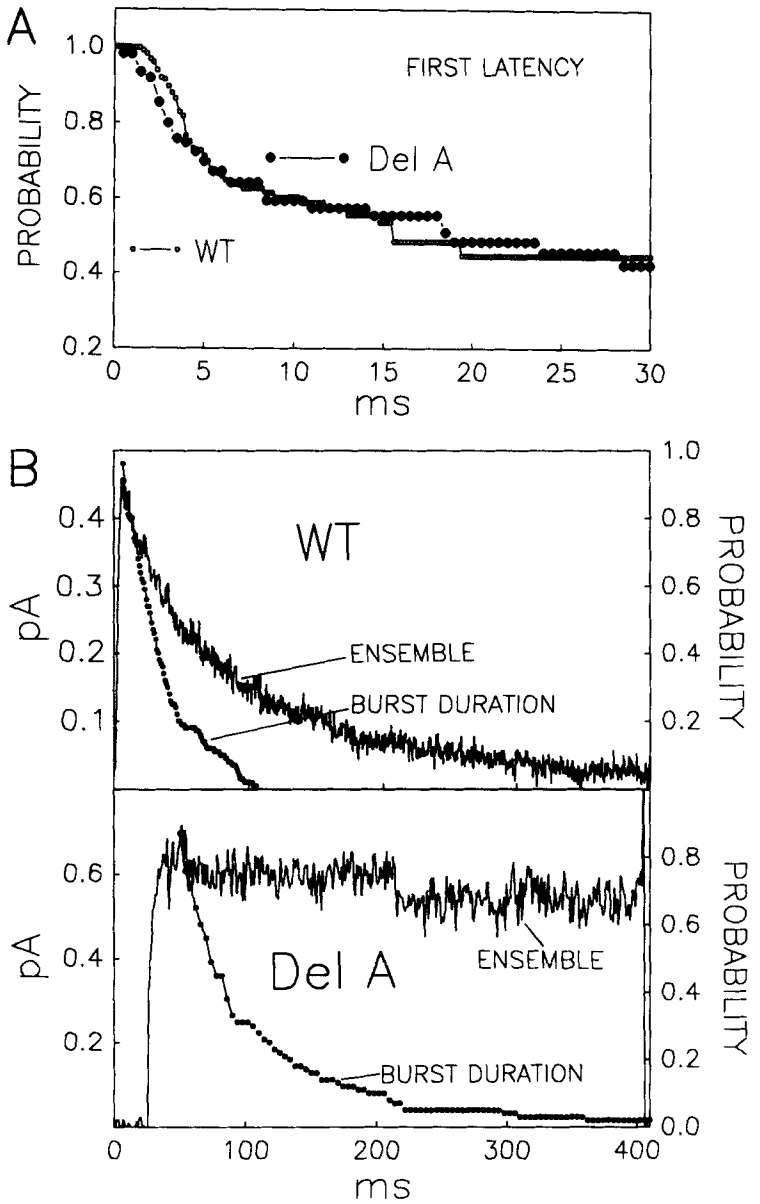

FIGURE 5. (*A*) Comparison between WT and Del A of the latency to first opening at +40 mV. Shown are the cumulative first latency distributions, which specify the probability of a first opening occurring later than the time on the abscissa. These distributions have been corrected for the number (*n*) of channels present in the patch (five for *WT* and three for *Del A*) by taking the *n*th root of the apparent distribution (Aldrich, Corey, and Stevens, 1983). (*B*) Comparison between the cumulative burst duration distributions (*right ordinates*) and ensemble averages (*left ordinates*) for WT (*top*) and Del A (*bottom*). Data were from the same patches as in *A*. The cumulative burst duration distributions specify the probability that a burst lasted longer than the time on the abscissa. A burst was defined as groups of openings that were separated by closed intervals shorter than or equal to a criterion duration. This criterion duration was set to five times the fastest time constant of closed time distribution of each patch, as described for Fig. 4 *B*. The cumulative burst duration distributions were shifted along the abscissa so that their beginnings match the peaks of the corresponding ensemble averages.

Del A was probably a greatly increased probability of channel reopening during depolarization. Due to the difficulty of finding patches containing only one channel, we could not quantify the reopening probability directly. However, such a difference between WT and Del A is suggested by the original single channel currents shown in Fig. 2. Fig. 5 *B* illustrates this point in a more quantitative manner. Here, we compared the cumulative burst duration distributions and the ensemble averages for both WT and Del A (Solc and Aldrich, 1990). For Del A, the ensemble average was maintained at about the same level throughout the duration of the pulse. Because the first latency rarely exceeded 30 ms (Fig. 5 *A*) and the burst duration rarely exceeded 200 ms, the wide separation between the burst duration distribution and the ensemble average at the end of the pulse can only be explained by a high probability of channel reopening during the pulse (Solc and Aldrich, 1990). On the other hand, for WT the separation between the ensemble average and the burst duration distribution was much smaller, indicating a lower probability of reopening of the WT channel during depolarization than that of Del A.

We conclude from the above that deleting domain A from RHK1 prolongs the burst duration and, more importantly, increases the probability of channel reopening during depolarization. These changes in single channel kinetics result in a marked reduction in the rate of decay of whole cell current. These are similar to the effects on channel kinetics of deleting or mutating the NH_2-terminal hydrophobic domain of *Shaker* H-4 (Hoshi et al., 1990), suggesting that domain A may form the hydrophobic portion of the ball in RHK1. We then examined the effects on channel function of deleting domain I which immediately follows domain A and contains net positive charges.

Effects of Deleting Domain I

Deleting domain I from RHK1 (Del I) reduced the rate of current decay (Fig. 6 *A, top*). The average $T_{1/2}$ of decay of Del I at +20 mV was 0.78 ± 0.18 s, 14 times that of WT (Fig. 6 *C, top*). Similar to WT, at 2 mM $[K]_o$ the restitution of Del I followed a single exponential time course (Fig. 6 *B, middle*). The average value of $T_{1/2}$ of restitution of Del I was 1.11 ± 0.36 s, significantly shorter than that of WT (Fig. 6 *C, middle*). Elevating $[K]_o$ from 2 to 20 mM accelerated the rate of Del I restitution (Fig. 6 *B, middle*). The degree of acceleration seemed to be lesser for Del I (67.0 ± 5.0% reduction in $T_{1/2}$ of restitution) than for WT (Fig. 6 *C, bottom*), although the difference did not reach statistical significance. Deleting domain I from RHK1 did not alter its voltage dependence of activation (Table II).

The slowing of current decay by deleting domain I from RHK1 was similar to the effect of deleting the positive charges from the ball of *Shaker* H-4 channel (Hoshi et al., 1990). This further supports the notion that there is a ball in RHK1 that consists of a hydrophobic portion (domain A) followed by a region of positive charges (domain I). The severity of alterations in channel function caused by deleting these two domains was not the same. The degree of reduction in the rate of current decay was much higher in Del A than in Del I: 110-fold vs 14-fold prolongation of $T_{1/2}$ of decay relative to WT. Similar to WT, the restitution of Del I was accelerated by elevating $[K]_o$. However, the restitution time course of Del A was not sensitive to external K ions. These observations suggest that deleting domain A may destroy the

function of the ball, and the extremely slow inactivation process of Del A may be mediated by a mechanism fundamentally different from that of WT. On the other hand, the inactivation of Del I may be mediated by a mechanism similar to that of WT, although the ball has been modified.

If deleting domain I modified but maintained the function of the ball, the positive charges of the modified ball in Del I were probably replaced by amino acids from the

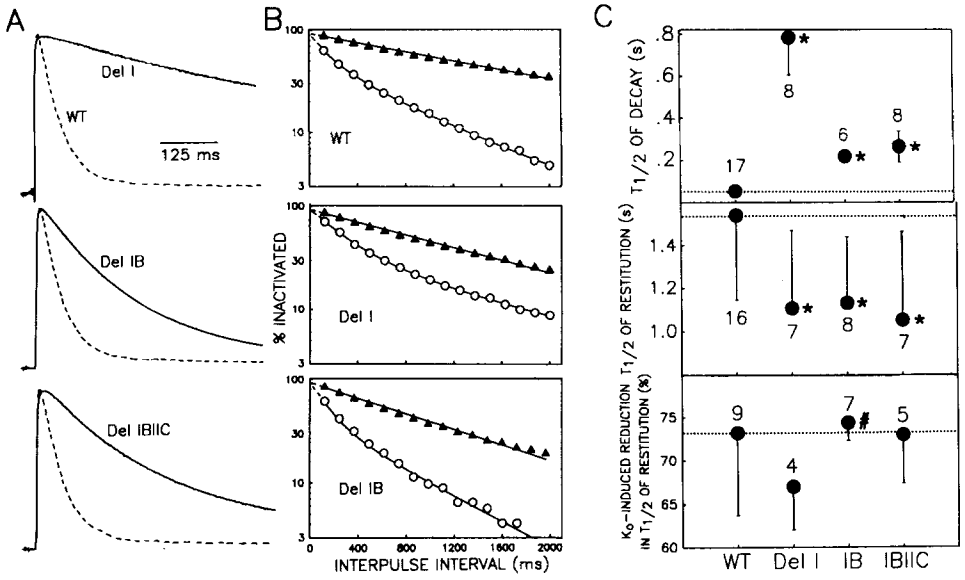

FIGURE 6. (*A*) Comparison of rate of decay between WT (*dotted traces*) and Del I, Del IB, and Del IBIIC. The voltage clamp protocol was as described for Fig. 1 *A*. (*B*) Comparison of the time courses of restitution between WT, Del I, and Del IB and the effects of elevating $[K]_o$ from 2 to 20 mM on restitution. The double-pulse voltage clamp protocols were similar to those described for Fig. 1 *B*. The duration of the double pulses was 2,000 ms for the deletion mutants and 500 ms for WT. Data obtained at 2 mM $[K]_o$ are denoted by filled triangles, while data recorded at 20 mM $[K]_o$ are shown as open circles. For all three channels, the restitution time courses at 2 mM $[K]_o$ were fitted with a single-exponential function, and those at 20 mM $[K]_o$ were fitted with a double-exponential function. The lines or curves superimposed on the data points were calculated from the appropriate function with the best-fit parameter values. (*C*) Comparisons between WT, Del I, Del IB, and Del IBIIC of their $T_{1/2}$ of decay at +20 mV (*top*), $T_{1/2}$ of restitution at 2 mM $[K]_o$ (*middle*) and % reduction in $T_{1/2}$ of restitution induced by elevating $[K]_o$ from 2 to 20 mM (*bottom*). Del IB and Del IBIIC are marked as "IB" and "IBIIC," respectively. Data analyses and figure format were as described for Fig. 1 *C*. WT data are the same as those shown in Fig. 1. $*P < 0.05$ relative to WT; $\#P < 0.01$ relative to Del I.

next region with a high density of positive charges (domain III). If this was the case, the hydrophobic portion of the modified ball in Del I would include domains A, B, II, and C. Its size (67 residues) would be substantially larger than that of WT (25 residues), although the change in the physical size of the ball is hard to predict because there is no data for the secondary structure of this region. The change in the size of the ball might destabilize the binding between the ball and its receptor due to

a steric hindrance (Isacoff et al., 1991). Moreover, the effective charge density of the modified ball may be reduced relative to that of WT, either due to an increase in the size of the hydrophobic portion (assuming that the hydrophobic portion formed a core protected from the aqueous environment by charged and hydrophilic residues, Hoshi et al., 1990), or due to an inefficient substitution of positive charges from domain III. This might also destabilize the binding between the ball and the receptor, if an electrostatic interaction is important for such a process. Either or both of these effects could account for the slowing of current decay and the acceleration of restitution in Del I relative to WT. Based on this hypothesis, deleting residues between domains A and III, and thus reducing the size of the ball, should reverse the effects of deleting domain I alone. Therefore, we deleted domain B or domains BIIC in addition to domain I, and examined the resulting effects on channel function. We made two predictions. First, Del IB and Del IBIIC should decay faster than Del I. Second, the effect of elevating $[K]_o$ on the restitution of Del IB and Del IBIIC should be stronger than that in Del I.

Effects of Deleting Domains IB, and IBIIC

Fig. 6 *A* compares the rates of current decay of Del IB and Del IBIIC with those of WT and Del I. For both Del IB ($T_{1/2}$ of decay 0.22 ± 0.03 s) and Del IBIIC (0.26 ± 0.07 s), the rate of decay was much slower than that of WT but significantly faster than that of Del I (Fig. 6 *C, top*). These observations are consistent with the first prediction. Elevating $[K]_o$ from 2 to 20 mM accelerated the rates of restitution of both Del IB and Del IBIIC (Fig. 6 *B* and *C, bottoms*). The degree of acceleration in Del IB (74.4 ± 2.1% reduction in $T_{1/2}$ of restitution) was significantly higher than that of Del I (67.0 ± 5.0%, $P < 0.01$). This is consistent with the second prediction. For Del IBIIC, the degree of acceleration (73.0 ± 5.6%) was also higher than that of Del I although the difference did not reach statistical significance. These data support our hypothesis that deleting domain I modified but maintained the function of the ball, and under this condition the positive charges from domain III could substitute for the like charges in domain I. However, for Del IBIIC although the hydrophobic portion of the ball contained only domain A (as in WT), the binding between the ball and the receptor was still less stable than in WT. The $T_{1/2}$ of restitution at 2 mM $[K]_o$ was 1.13 ± 0.31 s for Del IB and 1.05 ± 0.41 s for Del IBIIC. These values were significantly shorter than that of WT (Fig. 6 *C, middle*). The voltage dependences of activation of Del IB and Del IBIIC were similar to that of WT (Table II).

The top panel of Fig. 7 *A* illustrates the single channel currents of Del IB recorded at +40 mV. The channel opened and closed many times before entering a long-lived closed state. The interburst intervals were shorter than those of WT but much longer than those of Del A (compare Fig. 7 *A* with Fig. 2). The bottom panel of Fig. 7 *A* shows the ensemble average and the cumulative burst duration distribution from the same patch. The ensemble average decayed to 60% of its peak level at ~200 ms after the start of the depolarization pulse. Therefore similar to the whole cell currents, the rate of decay of the ensemble average of Del IB was intermediate between those of WT and Del A (compare Fig. 7 *A* and Fig. 5 *B*). The burst duration rarely exceeded 150 ms. The separation between the ensemble average and the cumulative burst duration distribution at the end of the pulse was most likely due to reopenings of Del

IB during depolarization. There was a 1.5-fold prolongation of the mean open time, and a 1.7-fold increase in the mean burst duration in Del IB relative to WT (Table III). Deleting domains IB did not affect the single channel current amplitude. Nor were there changes in the median first latency or the mean closed interval within bursts.

In the *Shaker* H-4 channel, it has been hypothesized that the 60 or so amino acids between the ball and the region conserved among members of the *Shaker* family constitute a chain (Fig. 1). Deleting 7 to 15 amino acids from the chain domain causes a graded acceleration of inactivation (Hoshi et al., 1990). Assuming that a

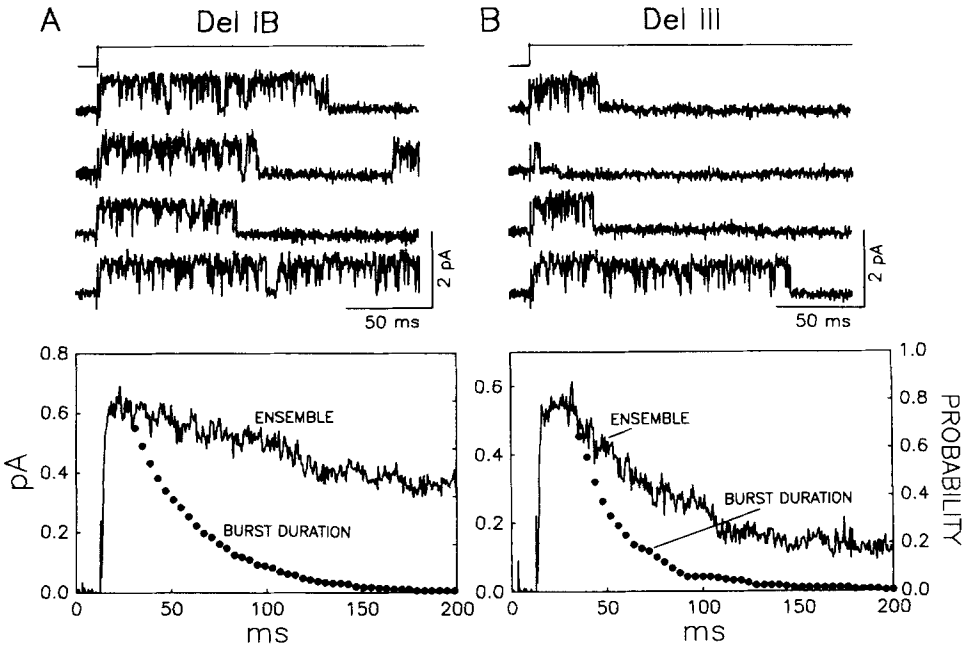

FIGURE 7. Single channel currents of Del IB (*A*) and Del III (*B*). The currents were recorded at +40 mV. The onset of the depolarization pulses is shown above. For each panel, four representative original current traces are shown on top, with a plot on the bottom comparing the ensemble average and the cumulative burst duration distribution from the same patch. Data analysis and figure format for the bottom plots are the same as those described for Fig. 5 *B*.

similar "chain" was present in RHK1, it would be composed of 136 residues between the ball (domains A and I) and the conserved region, i.e., domains B to E (Fig. 1). Deleting domains B, BII, IIC, D, and E did not affect the rate of current decay during depolarization (data not shown). We therefore tested whether deleting the remaining regions (domains III and IV) could increase the rate of current decay, thus confirming the presence of a "chain" in RHK1. Domain III contains 19 amino acids, with 1 negative and 11 positive charges. Domain IV is 26 amino acids in length, having 18 negative and 3 positive charges. The hydrophilic nature of these two domains resembles that of the chain in *Shaker* H-4. Furthermore, deleting domain III

or IV would cause a 14 or 19% shortening of the sequence of the hypothetical chain in RHK1. Based on data from *Shaker* H-4 (Hoshi et al., 1990), such changes might lead to a detectable acceleration of channel inactivation, although the physical length of the chain might not correspond to the length of the amino acid sequence due to secondary structures of this region.

Effects of Deleting Domain III or IV

Fig. 8 *A* and the top panel of Fig. 8 *C* show that deleting domain III slowed the rate of current decay ($T_{1/2}$ of decay: 0.14 ± 0.03 s), while deleting domain IV did not have appreciable effects on the time course of the current ($T_{1/2}$ of decay: 0.063 ± 0.016 s). These observations were not consistent with the existence of a chain in RHK1. These two deletions affected the rate of channel restitution differently. Deleting domain III accelerated the rate of restitution ($T_{1/2}$ of restitution: 0.94 ± 0.28 s), while deleting domain IV had an opposite effect (2.40 ± 1.16 s) (middle and bottom panels of Fig. 8 *B* and middle panel of Fig. 8 *C*). Furthermore, elevating $[K]_o$ accelerated the restitution of Del IV (78.4 ± 3.3% reduction in $T_{1/2}$ of restitution) significantly more than Del III (74.0 ± 3.2%) (Fig. 8 *C, bottom*). These results suggest that domains III and IV do not form a functional "chain" in RHK1. Deleting the positively charged domain III tended to reduce the stability of binding between the ball and its receptor, while deleting the negatively charged domain IV had an opposite effect. Deleting domain III or IV induced little or no changes in the voltage dependence of activation (Table II).

Fig. 7 *B* illustrates the single channel currents of Del III at +40 mV. Del III displayed a bursting behavior, similar to WT, Del A and Del IB. Deleting domain III did not affect the single channel current amplitude, the median first latency and the mean closed interval within bursts (Table III). There was a 1.6-fold prolongation of the mean open time and a twofold increase in the mean burst duration in Del III relative to WT (Table III). The bottom panel of Fig. 7 *B* compares the ensemble average and the cumulative burst duration distribution of Del III. At ~200 ms the ensemble average decayed to 25% of the peak level, and outlasted the burst duration which was ≤150 ms. This indicates that Del III could reopen during depolarization, but the probability was lower than that of Del IB (Fig. 7 *A*) or Del A (Fig. 5 *B*).

DISCUSSION

We studied the effects on channel function of deleting different domains from the NH_2 terminus of RHK1. The changes in channel function were quantified by analyzing both whole cell and single channel recordings. Combining these two approaches provides us with an opportunity to understand how channel gating is affected by different deletion mutations. We will first discuss the rationale for the measurements we made.

Experimental Design

We measured the rate of current decay during depolarization to infer the effects of NH_2-terminal deletions on the transition between the open and the inactivated states.

The time course of whole cell current is determined not only by the rates of transitions into and out of the open and inactivated states, but also by the rate of channel activation (Aldrich et al., 1983; Yue et al., 1989). Therefore, the rate of current decay should be measured at a sufficiently depolarized voltage so that the influence from the rate of channel activation could be minimized. We chose +20 mV

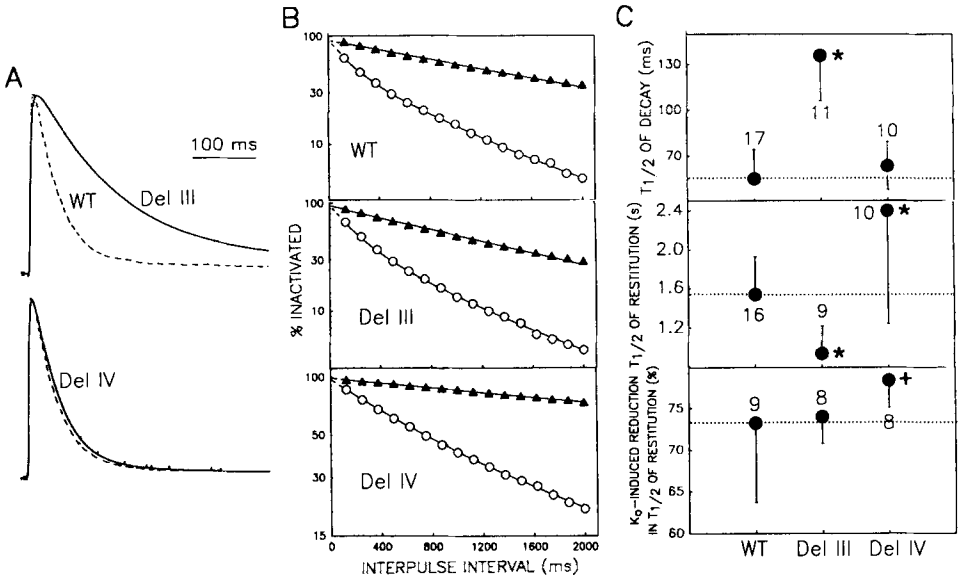

FIGURE 8. (*A*) Comparison of rate of decay between WT (*dotted traces*), Del III, and Del IV. The voltage clamp protocol was as described for Fig. 1 *A*. (*B*) Comparison of the time courses of restitution between WT, Del III, and Del IV and the effects of elevating $[K]_o$ from 2 to 20 mM on restitution. The double-pulse voltage clamp protocols were similar to those described for Fig. 1 *B*. The duration of the double pulses was 1000 ms for Del III and 500 ms for WT and Del IV. Data obtained at 2 mM $[K]_o$ are denoted by filled triangles, while data recorded at 20 mM $[K]_o$ are shown as open circles. The restitution time courses for WT and Del III at 2 mM $[K]_o$ and those of Del IV at both 2 and 20 mM $[K]_o$ were fitted with a single exponential function, while those of WT and Del III at 20 mM $[K]_o$ were fitted with a double exponential function. The curves or lines superimposed on the data points were calculated from the appropriate function with the best-fit parameter values. (*C*) Comparisons between WT, Del III, and Del IV of their $T_{1/2}$ of decay at +20 mV (*top*), $T_{1/2}$ of restitution at 2 mM $[K]_o$ (*middle*) and % reduction in $T_{1/2}$ of restitution induced by elevating $[K]_o$ from 2 to 20 mM (*bottom*). Data analyses and figure format are as described for Fig. 1 *C*. WT data are the same as those in Fig. 1. $*P < 0.05$ relative to WT; $+P < 0.01$ relative to Del III.

because at this voltage, the rate of decay of WT current approached a voltage-independent maximal level (manuscript submitted for publication). Due to the differences in the currents' time courses among various channels, the half-time of decay was used for comparison.

The rate of restitution is at least partially determined by the transition from the inactivated to the open states (Demo and Yellen, 1991). Therefore, this parameter

may provide some clues as to how NH_2-terminal deletions affect this transition step. Again, because the restitution time courses of these channels could not be described by a single unique function (Figs. 1, 6, and 8), the half-time of restitution was used for comparison. The time course of restitution was measured at a fixed holding voltage of −80 mV using a double-pulse protocol. The duration of the double pulses was adjusted according to the inactivation rate of the channel under study. This duration ranged from 0.5 to 5 s. We judged that these variations in pulse duration should not contribute to the differences in the restitution rate among channels we measured, based on the observation that the restitution time course of WT was not affected by changing the pulse duration from 0.05 to 0.5 or 5 s (Tseng and Tseng-Crank, 1992).

It has been shown for *Shaker* H-4 that elevating $[K]_o$ can accelerate the restitution process (Demo and Yellen, 1991). Based on the ball-and-chain hypothesis, this is explained by an electrostatic interaction between external K ions and the positively charged ball from the cytoplasm. Following this reasoning, it was hypothesized that if the effective charge density of the ball was altered by NH_2-terminal deletions, such a change might influence the interaction between external K ions and the ball. A reduction in the effective charge density of the ball may decrease the degree of high K_o-induced acceleration of restitution, while an increase in the charge density may have an opposite effect. Thus, we measured the restitution of each of the channels at 2 and 20 mM $[K]_o$, and compared the degrees of change in restitution (measured as % reduction in $T_{1/2}$ of restitution).

We analyzed single channel kinetics by grouping openings into bursts. An empirical method has been proposed to calculate an optimum criterion duration for defining bursts (Magleby and Pallotta, 1983). This method takes into account differences in the channel activity. This is comparable to our situation of having channels with different open probabilities after first opening. The calculation is based on the closed interval distribution: a criterion duration was calculated so that the probability of assigning interburst gaps to the category of intraburst intervals is equal to the probability of designating intraburst intervals as interburst gaps. The criterion duration calculated in this manner is typically 3–4 times the short time constant of the closed time distribution. However depending on the mechanism of channel gating, such a criterion duration may be shorter than the true interval between bursts and leads to an underestimation of the burst duration and the number of openings per burst (Magleby and Pallotta, 1983). In our experiments, there was another level of uncertainty due to the fact that in most of the patches we considered there were more than one active channel. This made the meaning of the slower components of closed time distributions uncertain. We set the criterion duration at five times the fastest time constant of the closed time distribution of each patch. The definition of bursts using such a criterion duration appeared to be satisfactory for WT, Del IB, and Del III, for which a clear distinction could be made between closed intervals within bursts and those between bursts (Fig. 2 *A*, and Fig. 7). For Del A, there might be an underestimation of the burst duration. For example, based on such a criterion duration the Del A patch shown in Fig. 2 *B* had a mean burst duration of 56 ms and, on average, 14 openings per burst. Obviously, some bursts lasted much longer than this estimation. However, this should not alter our conclusion that the average burst duration of Del A is longer than that of the WT channel.

Effects of NH_2-terminal Deletions on the Function of RHK1

We will discuss our results based on the following gating scheme modified from that of Zagotta and Aldrich (1990) for a *Shaker* (A_1) channel.

$$C_1 \underset{\beta_1}{\overset{\alpha_1}{\rightleftarrows}} C_2 \rightleftarrows \cdots \rightleftarrows C_{n-1} \underset{\beta_{n-1}}{\overset{\alpha_{n-1}}{\rightleftarrows}} C_n \underset{\lambda}{\overset{\kappa}{\rightleftarrows}} O \underset{\delta}{\overset{\gamma}{\rightleftarrows}} I$$

C, *O*, and *I* denote the closed, open and inactivated states, respectively. In this scheme, the channel needs to traverse a number of closed states before opening. This is consistent with the initial delay in the first latency distributions (Fig. 5 *A*). The transitions between these closed states are governed by voltage-dependent rate constants, labeled as α_i and β_i (i = 1 to n − 1). In the voltage range where the degree of channel activation approaches a plateau ($\geq$ +20 mV), the rate of current decay of the WT channel reaches a voltage-independent maximal level (manuscript submitted for publication). This suggests that the transitions into and out of the open and inactivated states have little or no voltage-dependence. After the first opening, the channel closes and opens several times (bursts) before entering a long-lived closed state. The above gating scheme assumes that bursts result from transitions between *O* and a nearby closed state in the activation pathway, C_n. This is consistent with the observation that the mean closed interval within bursts (0.3–0.4 ms) is much shorter than the median first latency (3–4 ms, Table III). Bursts are terminated by entering the *I* state.

The similarity in the single channel current amplitudes between WT, Del A, Del IB, and Del III suggests that the NH_2-terminal region of RHK1 is not involved in the ion permeation process of the channel (Table III). The activation curves of the deletion mutants were similar to that of WT, indicating that the NH_2-terminal region probably does not participate in the voltage-dependent activation process of the channel (Table II). This is also supported by the observation that the first latency was not different between WT, Del A, Del IB, and Del III (Table III). Based on the above gating scheme, the mean closed interval within bursts (t_c) should be equal to the reciprocal of the sum of rate constants of transitions out of C_n (Colquhoun and Hawkes, 1983): $t_c = 1/(\kappa + \beta_{n-1})$. Our single channel measurements were made at +40 mV. At this voltage, the value of β_{n-1} was most likely negligible due to its voltage-dependence. Therefore, t_c could be approximated by:

$$t_c = 1/\kappa. \tag{1}$$

The lack of differences in t_c (and thus the rate constant, κ) among WT, Del A, Del IB, and Del III suggests that NH_2-terminal deletions did not affect the transition from C_n to *O*.

Based on the above scheme, there should be a predictable relationship between the mean open time within bursts (t_o) or the mean burst duration (D_b) and the rate constants governing the transitions into and out of *O* and *I* (Colquhoun and Hawkes, 1983):

$$t_o = 1/(\lambda + \gamma) \tag{2}$$

$$D_b = [1 + (\lambda/\kappa)]/\gamma. \tag{3}$$

The values of λ and γ could be calculated from t_o and D_b according to these equations, along with "κ" from Eq. 1. The calculated values of these parameters for WT, Del III, Del IB, and Del A are listed in Table IV. There is a reduction in the rate constant for the transition from O to I (γ), most likely caused by a modification of the function of the ball by these NH_2-terminal deletions. However, the reduction in "γ" alone could not totally account for the slowed decay of whole cell current in all the mutant channels. This is illustrated by a comparison of the prolongation of $T_{1/2}$ of decay and D_b among Del III, Del IB, and Del A relative to WT (Fig. 9). For Del III, the prolongation of $T_{1/2}$ of decay was largely due to the increase in D_b. However, for

TABLE IV

Parameters Used for Simulating Currents of the Wild-Type RHK1 (WT) and Deletion Mutant Channels

	WT	Del A	Del IB	Del III
A_α (s^{-1})	230	230	230	230
A_β (s^{-1})	20	20	20	20
V_α (mV)	70.3	70.3	70.3	70.3
V_β (mV)	14.6	14.6	14.6	14.6
κ (s^{-1})	2778	3125	2941	3125
λ (s^{-1})	642	503	436	420
γ (s^{-1})	71.9	23.6	39.8	34.5
δ (s^{-1})	1	111	12.5	2.5

The above parameter values were used to calculate the time courses of currents of the wild-type RHK1 (*WT*) and deletion mutant channels according to the following state-diagram and equations:

$$C_1 \underset{\beta}{\overset{4\alpha}{\rightleftarrows}} C_2 \underset{2\beta}{\overset{3\alpha}{\rightleftarrows}} C_3 \underset{3\beta}{\overset{2\alpha}{\rightleftarrows}} C_4 \underset{4\beta}{\overset{\alpha}{\rightleftarrows}} C_5 \underset{\lambda}{\overset{\kappa}{\rightleftarrows}} O \underset{\delta}{\overset{\gamma}{\rightleftarrows}} I$$

$$\alpha = A_\alpha \exp(V/V_\alpha) \quad (4)$$

$$\beta = A_\beta \exp(-V/V_\beta). \quad (5)$$

Simulation was for V_h −80 mV and a voltage step to +20 mV. The steady state probabilities of distribution of channels in different states at −80 mV was first calculated. This was followed by integration of differential equations based on the above scheme for V = +20 mV using a fourth order Runge-Kutta subroutine provided by QuickPak Scientific (Crescent Software, Crescent Scientific Equipment Corp., Long Beach, CA). For each of the channels, the values of κ, λ, and γ were calculated using the average values of mean closed time within bursts (t_c), mean open time (t_o), and mean burst duration (D_b) from single channel recordings at +40 mV based on Eqs. 1–3 (see text).

Del IB the degree of prolongation of $T_{1/2}$ of decay exceeded that of D_b. This difference was even more prominent in Del A. Therefore, some other factor(s) might also make important contribution to the prolongation of $T_{1/2}$ of decay beside a reduction in γ. A comparison of the ensemble averages and the cumulative burst duration distributions of WT, Del III, Del IB, and Del A (Figs. 5 *B* and 7) suggests that the probability of channel reopening during depolarization was different among these channels. The order of increasing reopening probability is: WT < Del III < Del IB < Del A. According to the above gating scheme, the probability of reopening during depolarization is determined by the rate constant δ. Our observations thus

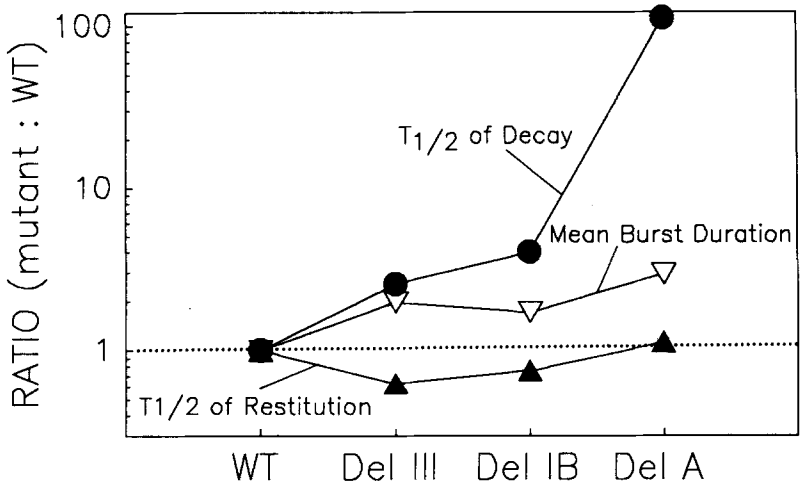

FIGURE 9. Comparison between WT, Del III, Del IB, and Del A of their $T_{1/2}$ of decay, $T_{1/2}$ of restitution, and mean burst duration. The ratios of average values of these parameters of the mutant channels to those of the wild-type channel (*mutant:WT*) are plotted on a logarithmic scale. For the sake of clarity, the symbols are connected by lines.

suggest that deleting domains III, IB, and A induced a graded enhancement of transition from the *I* to the *O* states. Fig. 10 shows simulated current traces of WT, Del III, Del IB, and Del A based on a kinetic model modified from the above general scheme (see Table IV legend). The assumed parameter values that determine the voltage-dependence of channel activation (A_α, A_β, V_α, V_β) are the same for all these channels, while the assumed values of δ vary greatly among them (Table IV). The simulations largely reproduce the qualitative features of the whole cell and ensemble average currents of WT, Del III, and Del A (Figs. 1 *A*, 2, 7 *B* and 8 *A*). For Del IB, the simulated current shows a more distinct biphasic nature than that of the experimental observations (Figs. 6 *A* and 7 *A*).

Since the restitution process is at least partially determined by the transition from I to O (Demo and Yellen, 1991), its rate should be accelerated by NH_2-terminal deletions that increased the rate constant "δ." Indeed, the restitution of Del I, Del IB, Del IBIIC, and Del III was faster than that of WT (Figs. 6 and 8). However, this was

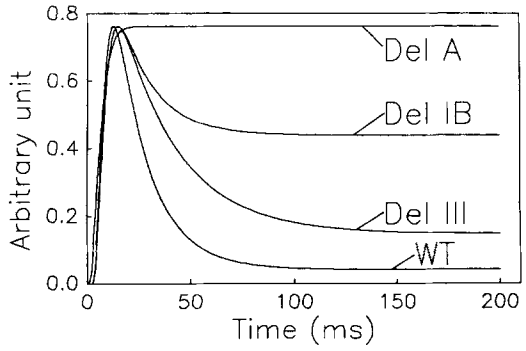

FIGURE 10. Simulation of currents of WT, Del III, Del IB, and Del A. The parameters used for simulation are listed in Table IV. The state diagram and equations for calculation are given in the legend of Table IV.

not the case for Del A (Fig. 1). The apparent discrepancy between Del A and the other mutant channels (Fig. 9) may be explained by the possibility that while the inactivation of the other mutant channels was mediated by a mechanism similar to that of the WT channel, the inactivation of Del A was fundamentally different.

The slowed restitution of Del IV relative to WT suggests that the rate of transition from *I* to *O* may be reduced in this deletion mutant. Elevating $[K]_o$ accelerated the restitution of Del IV to a higher degree than that of Del III or WT (Fig. 8). Deleting domain IV should increase the net positive charges in the NH_2 terminus of RHK1. These observations suggest that in the WT channel the negative charges of domain IV may decrease the effective charge density of the ball, and reduce the stability of binding between the ball and its receptor.

Structural Implications

Our experiments suggest that the NH_2 terminus of RHK1 may be similar to that of *Shaker* H-4 (Hoshi et al., 1990; Zagotta et al., 1990) in having a ball composed of a hydrophobic region (domain A) and a hydrophilic region with predominantly positive charges (domain I). Deleting domain A appeared to abolish the function of the ball. Deleting domain I modified but maintained the function of the ball. There does not seem to be a rigid structural requirement for the ball in RHK1. The hydrophobic region may be formed by domain A or by a combination of domains A, B, II, and C. The positive charges may be donated by domain I and, to a lesser degree, by domain III. Our data also suggest that the positive charges in domain III and the negative charges in domain IV both influence the stability of binding between the ball and its receptor, probably by affecting the effective charge density of the ball. We could not identify a chain in the NH_2 terminus of RHK1, as has been proposed for *Shaker* H-4 (Hoshi et al., 1990). The cytoplasmic NH_2-terminal region of RHK1 is important in determining the channel properties related to inactivation, but is not involved in the activation or ion permeation process.

The authors would like to thank Dr. P. K. Wagoner for discussion of data and helpful suggestions. The authors also want to thank Shulamith Hazum and Holly King for their technical support, and Dr. Shiun Ling for helping with the model simulation.

This study was supported by HL-08508 from National Heart, Blood and Lung Institute, National Institute of Health, Bethesda, MD, and by a Grant-in-Aid from American Heart Association/New York City Affiliate and an Established Investigatorship from American Heart Association to Gea-Ny Tseng.

Original version received 19 May 1993 and accepted version received 26 August 1993.

REFERENCES

Aldrich, R. W., D. P. Corey, and C. F. Stevens. 1983. A reinterpretation of mammalian sodium channel gating based on single channel recording. *Nature.* 306:436–440.

Armstrong, C. M., and F. Bezanilla. 1977. Inactivation of the sodium channel II. Gating current experiments. *Journal of General Physiology.* 70:567–590.

Bolton, R., N. Dascal, B. Gillo, and Y. Lass. 1989. Two calcium-activated chloride conductances in *Xenopus laevis* oocytes permeabilized with the ionophore A23187. *Journal of Physiology.* 408:511–534.

Chandy, K. G. 1991. Simplified gene nomenclature. *Nature.* 352:26–26.

Colquhoun, D., and A. G. Hawkes. 1983. The principles of the stochastic interpretation of ion channel mechanisms. *In* Single Channel Recording. B. Sakmann and E. Neher, editors. Plenum Publishing Corp., New York. 135–175.

Colquhoun, D., and F. J. Sigworth. 1983. Fitting and statistical analysis of single channel records. *In* Single Channel Recording. B. Sakmann and E. Neher, editors. Plenum Publishing Corp., New York. 191–263.

Demo, S. D., and G. Yellen. 1991. The inactivation gate of the *Shaker* K^+ channel behaves like an open channel blocker. *Neuron.* 7:743–753.

Hamill, O. P., A. Marty, E. Neher, B. Sakmann, and F. J. Sigworth. 1981. Improved patch clamp techniques for high resolution current recordings from cells and cell-free membrane patches. *Pflugers Archiv.* 391:85–100.

Hoshi, T., W. N. Zagotta, and R. W. Aldrich. 1990. Biophysical and molecular mechanisms of *Shaker* potassium channel inactivation. *Science.* 250:533–538.

Isacoff, E. Y., Y. N. Jan, and L. Y. Jan. 1991. Putative receptor for the cytoplasmic inactivation gate in the *Shaker* K^+ channel. *Nature.* 353:86–90.

Kunkel, T. A. 1985. Rapid and efficient site specific mutagenesis without phenotypic selection. *Proceedings of the National Academy of Sciences.* 82:488–492.

Liebovitch, L. S., L. Y. Selector, and R. P. Kline. 1992. Statistical properties predicted by the ball and chain model of channel inactivation. *Biophysical Journal.* 63:1579–1585.

Magleby, K. L., and B. S. Pallotta. 1983. Burst kinetics of single calcium-activated potassium channels in cultured rat muscle. *Journal of Physiology.* 344:605–623.

Methfessel, C., V. Witzemann, T. Takahashi, M. Mishina, S. Numa, and B. Sakmann. 1986. Patch clamp measurements on *Xenopus laevis* oocytes: currents through endogenous channels and implanted acetylcholine receptor and sodium channels. *Pflugers Archiv.* 407:577–588.

Solc, C. K., and R. W. Aldrich. 1990. Gating of single non-*Shaker* A-type potassium channels in larval *Drosophila. Journal of General Physiology.* 96:135–165.

Stocker, M., W. Stuhmer, R. Wittka, X. Wang, R. Muller, A. Ferrus, and O. Pongs. 1990. Alternative *Shaker* transcripts express either rapidly inactivating or noninactivating K^+ channels. *Proceedings of the National Academy of Sciences, USA.* 87:8903–8907.

Tseng, G.-N., and J. Tseng-Crank. 1992. Differential effects of elevating $[K]_o$ on three transient outward K channels: Dependence on channel inactivation mechanism. *Circulation Research.* 71:657–672.

Tseng-Crank, J., G.-N. Tseng, A. Schwartz, and M. A. Tanouye. 1990. Molecular cloning and functional expression of a potassium channel cDNA isolated from a rat cardiac library. *FEBS Letters.* 268:63–68.

Yao, J.-A., J. Tseng-Crank, L. Lipka, M. F. Berman, and G.-N. Tseng. 1992. Comparison of a mammalian cardiac transient outward K channel, RHK1, with its N_2-terminal deletion mutant at whole-cell and single channel levels. *Circulation.* 86:I–77.

Yue, D. T., J. H. Lawrence, and E. Marban. 1989. Two molecular transitions influence cardiac sodium channel gating. *Science.* 244:349–352.

Zagotta, W. N., and R. W. Aldrich. 1990. Voltage-dependent gating of *Shaker* A-type potassium channels in drosophila muscle. *Journal of General Physiology.* 95:29–60.

Zagotta, W. N., T. Hoshi, and R. W. Aldrich. 1990. Restoration of inactivation in mutants of *Shaker* potassium channels by a peptide derived from ShB. *Science.* 250:568–571.